FATIGUE BEHAVIOUR OF AA6082-T6 ALUMINIUM ALLOY FRICTION STIR WELDS UNDER VARIABLE AMPLITUDE LOADING

J.D. Costa[1], J.A.M. Ferreira[1] and L.P. Borrego[2]

[1] CEMUC, Mechanical Engineering Department,
University of Coimbra, Rua Luís Reis Santos, Pinhal de Marrocos, 3030-788, Coimbra, Portugal.
E-mail: jose.domingos@dem.uc.pt.; martins.ferreira@dem.uc.pt.

[2] CEMUC, Mechanical Engineering Department,
Polytechnic Institute of Coimbra, Quinta da Nora - 3030, Coimbra, Portugal.
E-mail: borrego@isec.pt.

ABSTRACT

In addition to uncertainty such as material strength, notch geometries, defect contents and residual stresses, welded components are often subjected to variable amplitude service loads. In the case of friction stir welding of aluminium alloys, no data is available concerning fatigue behaviour under variable amplitude loading. The objective of this investigation is to determine the fatigue strength of friction stir welds in AA6082-T6 under constant and variable amplitude loading and analyse the validity of Miners´s rule in this specific welding process. Fatigue tests were carried out in a servo-hydraulic testing machine using stress ratios of R = 0 and R=-1. Typified Gassner amplitude spectra were considered, using four values for the shape exponent. Microhardness tests were performed to characterize the Vickers hardness profile in the vicinity of the weld area. Friction stir welding process leads to a decrease of the static mechanical properties relatively to base material. Detailed examination revealed a hardness decrease in the thermo mechanically affected zone and the nugget zone average hardness was found to be significantly lower than the base alloy hardness. Welded specimens show significantly lower lives than base material specimens. For the welded specimens tested at a stress ratio R=0 a good agreement was observed between constant and variable fatigue loading, using the equivalent stress calculated by Miner´s rule. For R=-1, Miner´s rule seems to overestimate the fatigue life.

KEY WORDS: Friction Stir Welding, aluminium alloy, fatigue, variable amplitude loading.

1. INTRODUCTION

Friction stir welding (FSW) is a relatively new solid-state joining process and is very energy efficient, environment friendly, and versatile, being considered to be the most significant development in metal joining in a decade. Since its invention in 1991 at the Welding Institute (TWI) of UK [1], a large amount of research was carried out in several fields and different materials. Aluminium alloys are the materials more often studied and where this technique has shown a better performance. Comparative mechanical properties studies of base material and welded specimens, including fatigue strength tests have been performed by several authors [2-6].

In addition to uncertainty such as material strength, notch geometries, defect contents and residual stresses, welded components are often subjected to variable amplitude service loads. The lack of Miner´s validity accumulation rule [7] has been demonstrated in many applications and, in consequence, its usage will introduce uncertainties which must be compensated by safety factors. In the case of friction stir welding (FSW) no data is available concerning fatigue behaviour under variable amplitude loading

The objective of this work is to study the fatigue strength of friction stir welds under constant and variable amplitude loading and analyse the validity of Miners´s rule for this specific welding process**.**

2. EXPERIMENTAL DETAILS

2.1 Preparation of welds

This research was conducted using the AA6082 aluminium alloy with a T6 heat treatment. The T6 heat treatment corresponds to a conversion of heat-treatable material to the age-hardened condition by solution treatment, quenching and artificial age-hardening. The alloy chemical composition and mechanical properties are shown in Tables 1 and 2, respectively.

The friction stir welds were performed in an aluminium plate with 4 mm thickness using a tool with a 5 mm diameter threaded pin and the shoulder had 16 mm diameter.

Table 1 - Chemical composition of AA6082-T6 aluminium alloy (wt%)

Si	Mg	Mn	Fe	Cr	Cu	Zn	Ti	Other
1.05	0.8	0.68	0.26	0.01	0.04	0.02	0.01	0.05

Table 2 - Mechanical properties of AA6082-T6 aluminium alloy

Tensile strength, σ_{UTS} (MPa)	300
Yield strength, σ_{YS} (MPa)	245
Elongation, ε_r (%)	9
Hardness, Hv,02	110

Welding parameters depend on several factors, namely, alloy type, penetration depth and joint. The following parameters were chosen in order to obtain welds with a good surface aspect and where no defects could be identified by microscopic observation: welding speed of 300 mm/min, tilt angle of 2º; rotating speed of 1500 rpm. Figure 1 is an example of the better succeeded welds concerning its surface aspect. In this weld sample, also a good penetration control of the shoulder was obtained. This is a very important aspect, because an excessive penetration will create a notch effect that could affect mainly the fatigue strength.

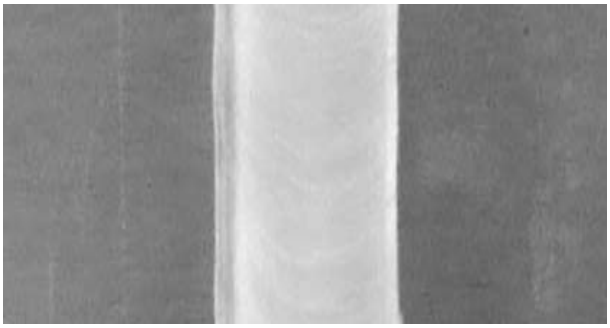

Figure 1. Surface aspect of a friction stir weld.

The penetration depth was adapted to fully penetrated butt joint. From each welded plate, the first 40 mm of the plate were not used in specimens preparation, in order to exclude possible deviation from steady state due to the typical lower temperatures during welding start. In order to analyse that no defects like root flaws, tunnel or kissing bond defects were present in the welds, cross-sectioning of the welds for metallographic analysis in planes perpendicular to the welding direction were also performed. The samples were prepared accordingly to standard metallographic practice and etched in order to enable the identification of the different weld zones. Figure 2a shows an example of a poor quality welded plate, presenting a tunnel defect size of about 0,6 mm, obtained before welding parameters optimization, while figure 2b shows the cross section of a welded plate welded with the parameters above referred, where no defects were observed by microscopy observation. The tunnel defects tend to appear in the advancing side of the nugget lower zone near the thermo-mechanically affected zone and they are continuously formed in the weld direction. The size of these defects tends to be great at the start of the welding process due to lower temperature generally achieved.

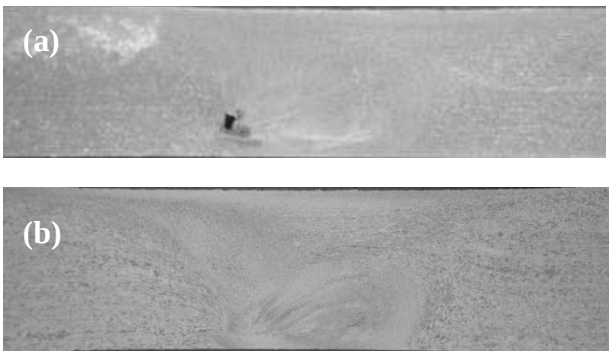

Figure 2. a) weld presenting a defect type tunnel; b) weld without defects identifiable by microscopy.

The majority of welds performed with only one passage leads to the presence of a tunnel defect formed mainly in the retracting side. Although, in some cases the tunnel defects observed had a size smaller than 30 μm, which did not influence static mechanical properties, the fatigue resistance was significantly affected. One way to avoid tunnel defects is increasing heat input by applying a higher axial force. However, an excess of axial force leads the formation of shear lips in the upper surface, creating stress concentration which also reduces fatigue live. It was realized to be very difficult to perform the correct optimization of all parameters. Therefore, to avoid the presence of the tunnel defects some welds were performed with two passages.

2.2 Fatigue details

Fatigue tests were carried out in a servo-hydraulic testing machine under constant and variable amplitude loadings. The dimensions of the fatigue specimens were 160x15x4 mm^3 (length, width, thickness). The cut specimens (Fig. 3) were milled at the edges, and weld surface preparation was made only by grind removing the thickness exceeding material.

Figure 3. Photo of a fatigue specimen cut from welded plate before edges machining.

Specimens machined of plates where defects were identified, typically tunnel defects with less than 200 μm, were also tested in order to evaluate their influence on fatigue resistance. The weld was transverse to the stress axis in the S–N tests and to the material rolling direction. A sinusoidal load–time function was used, with the stress ratio *R* set to 0 and -1. The frequency was in the interval of 20–40 Hz depending upon the stress level. Life was defined as the number of cycles to

failure and a total of 57 specimens were tested. For the variable loading amplitude tests, typified amplitude spectra [8], according to equation 1, were considered, using four values for the shape exponent ν, namely, 1,5, 2, 4 and 5,

$$log\, H_i = \left[1 - \left(\frac{S_{a,i}}{S_{a,max}}\right)^{\nu}\right] log\, H_0 \quad (1)$$

where

H_i cumulative frequency of load cycles for level $S_{a,i}$
H_0 block size (number of cycles)
ν shape exponent

Equation 2 specifies an additional number, the 'spectrum shape factor', *SSF*, that represents the distance (factor, life ratio) between an (arbitrary) Wohler S–N curve and the associated spectrum fatigue life curve (in Germany sometimes referred to as Gassner curve in honour of Ernst Gassner).

$$SSF = log \frac{\sum n_i}{\sum n_i \left(\frac{S_{a,i}}{S_{a,max}}\right)^m} \quad (2)$$

Using the loading spectrum defined by equation 1, *SSF* can be more precisely calculated using the following equation

$$SSF = log \frac{H_o}{\int_0^1 \frac{d}{dx}\left[-H_o{}^{(1-(x)^{\upsilon})}\right] \cdot (x)^m dx} \quad (3)$$

where, $x = \frac{S_a}{S_{a,max}}$ (4)

SSF depends on the shape of the spectrum under consideration (parameters H_0 and ν) and the slope, m, of Wohler´s curve. Table 3 present *SSF* values for some ν values and a description of its typical applications. This factor was calculated using the Miner damage rule (without endurance limit), taking $H_0=10^6$ cycles and m=5,5

Table 3. Spectrum shape parameters ν and SSF for typified amplitude spectra: $H_0=10^6$; m=5,5.

v	**SSF**	**Description**
∞	0	Constant amplitude loading
5	1,30	
4	1,56	ν>2 typical of bridge and crane structures
2	2,61	Stationary Gaussian process
1,5	3,14	
1	3,95	Typical for road roughness induced loads
0,8	4,39	ν<1 typical for wind gusts, wave actions, etc.

Figures 4 and 5 show the several variable loading amplitude spectra applied during fatigue tests. Figure 4 is the typical form of spectrum presentation where the normalized stress amplitude is plotted against the cumulative number of cycles, while in figure 5 a more intuitive way for spectrum interpretation is shown, depicting the number of cycles versus the normalized stress amplitude.

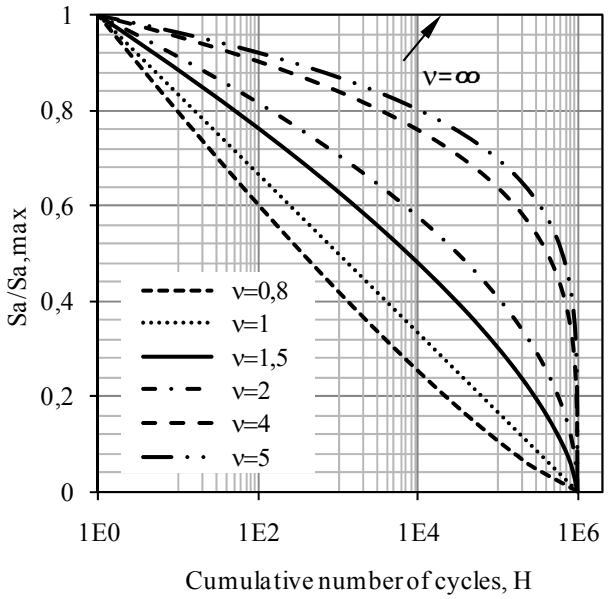

Figure 4. Typified amplitude spectra: normalized stress amplitude versus cumulative number of cycles ($H_0=10^6$ cycles).

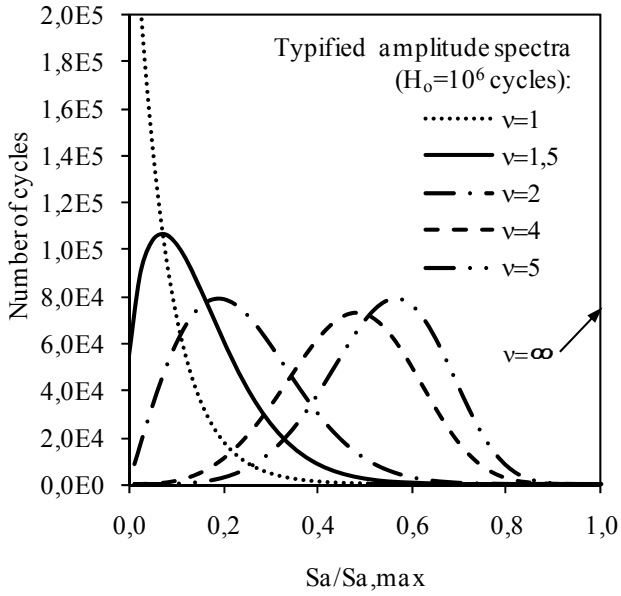

Figure 5. Typified amplitude spectra: number of cycles versus the normalized stress amplitude.

2.3 Microhardness details

Microhardness tests were performed to characterize the Vickers hardness profile in the vicinity of the weld area using a 2 N load. Measurements were performed along three lines: 0,5 mm far from both surfaces and at the

specimen middle thickness, in successive positions with 1 mm of distance.

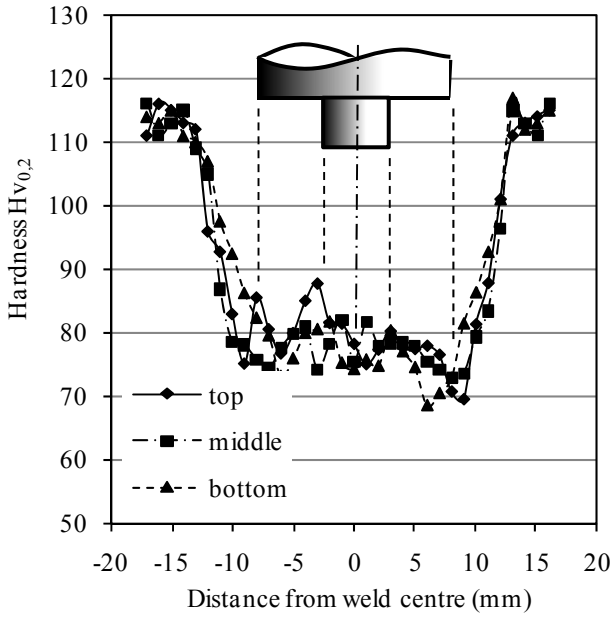

Figure 6. Hardness profiles measured along three lines.

This figure shows clearly a hardness decrease in the thermo mechanically affected zone and that the nugget zone average hardness is significantly lower than the base alloy hardness. Hardness profiles were measured in all plates. Microstructures hardness of the welds typically ranged between 70 and 80 $HV_{0,2}$, leading to a softening up to 60% relatively to the base material hardness (about 115 $HV_{0,2}$). The results show similar hardness profiles for the three measurement lines, although bottom measurements show that the lower hardness is restricted to a shorter zone.

3. RESULTS

Table 4 shows the mechanical properties of welded specimens obtained in tension tests. Compared with base material (table 2), friction stir welding process leads to a decrease of the material mechanical properties: yield and rupture stresses of friction welded specimens are significantly lower than for base material. Yield stress decreases 33% and the rupture stress decreases 20% relatively to base material values.

Table 4 - Mechanical properties of friction stir welds performed in AA6082-T6 aluminium alloy.

Tensile strength, σ_{UTS} (MPa)	241
Yield strength, σ_{YS} (MPa)	165
Elongation, ε_r (%)	6,8

Fatigue results obtained for the stress ratio R=0 under constant and variable amplitude loadings are plotted in figure 7. Fatigue data for constant amplitude loading were statistically analysed accordingly ASTM E739-91 Standard [9]. A low dispersion of fatigue data was obtained: the standard deviation was 0,04 for stress and 0,21 for fatigue life. This is a lower dispersion when compared with fatigue data obtained in tests of specimens welded by other processes. Fatigue data obtained with variable amplitude loading, using the equivalent stress range calculated accordingly to Miner´s rule, are in the same scatter band of the constant amplitude loading results, indicating that Miner´s rule gives real damage sum values near unity. The damage sum D ranged between 0,6 and 2 for the four spectra loadings. This conclusion is better visible in Figure 8 where the probability of occurrence is plotted against real damage sum values.

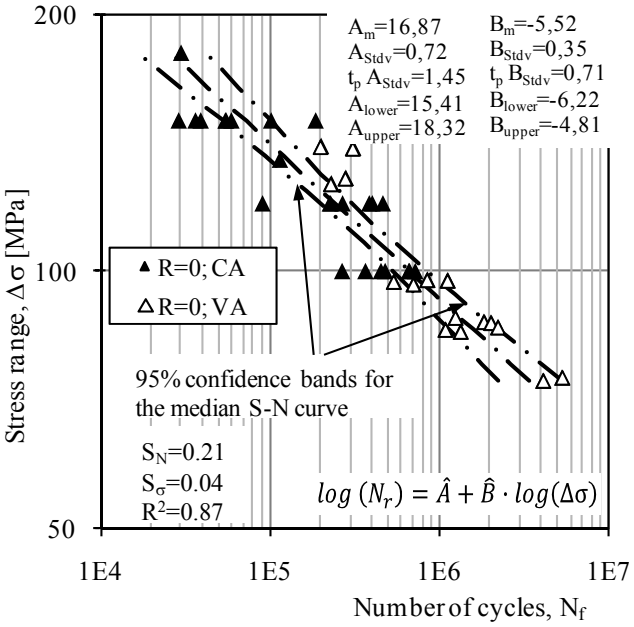

Figure 7. Wohler curves for R=0. Constant and variable amplitude loadings.

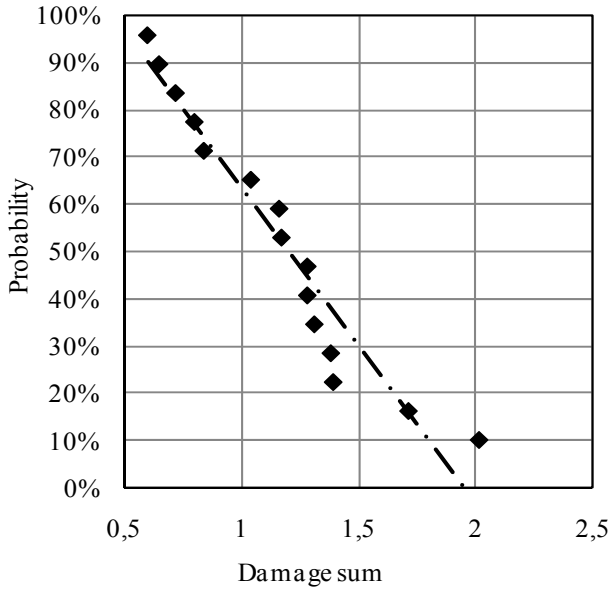

Figure 8. Real damage sum distribution.

Figure 9 compares fatigue results obtained with constant and variable amplitude loadings for the stress ratios R=0 and R=-1, plotting stress range against the number of cycles to failure. Data for variable amplitude loading and R=-1 were restricted to the shape exponent ν=2.

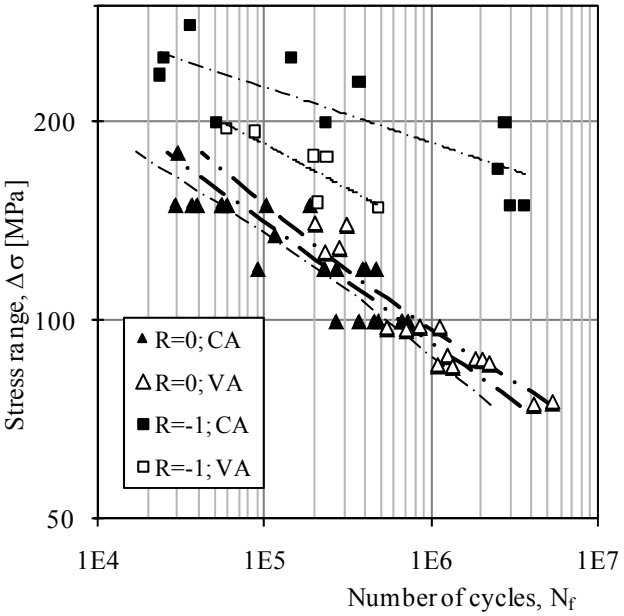

Figure 9. Wohler curves for R=0 and R=-1. Constant and variable amplitude loadings.

As expected, a significant influence of the mean stress was observed: for the same stress range, specimens tested with R=-1 present higher lives than specimens tested with R=0. For R=-1 fatigue data obtained under variable amplitude present lower lives than under constant amplitude loading, indicating that damage sum values are lower than unity for the majority of the tests. Therefore, Miner´s rule seems to overestimate the fatigue life in the case of the stress ratio of R=-1. More tests are in course under variable amplitude loading for R=-1 and other spectrum shape exponents in order to confirm this trend.

Figure 10 shows the Wohler curve (stress range versus life) and Gassner curves (spectrum maximum stress range versus life) for R=0 and for several values of the spectrum shape exponent, ν. The graphical meaning of the *SSF* parameter is also indicated. It is clear that as ν increases the Gassner curve becomes more close to Wohler curve. As referred before *SSF*=1 when $\nu=\infty$.

Figure 11 compares fatigue results obtained in this work for R=0 under constant amplitude loading with results obtained by other authors [1,3] in welded specimens of the same alloy. S-N curves obtained with specimens welded by FSW, MIG and TIG processes as well as base material are superimposed in the figure for comparison. Design curve for full-penetration both-sided butt joint accordingly to Eurocode 9 (class 35-4) is also depicted in the figure.

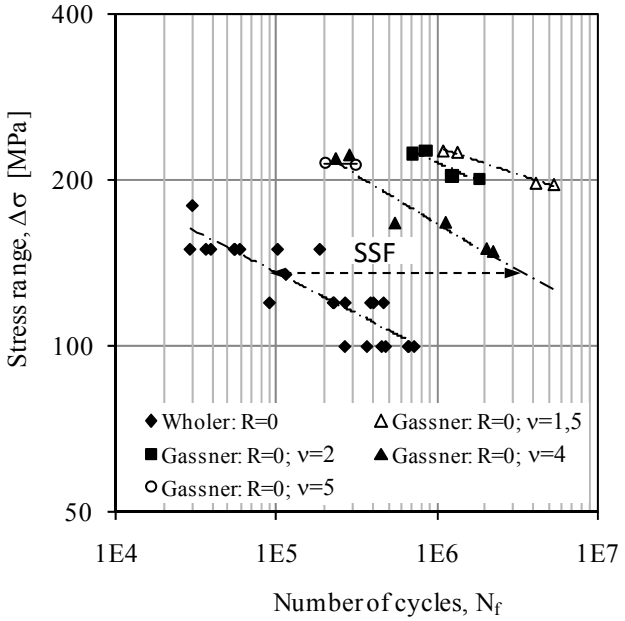

Figure 10. Wohler and Gassner curves for R=0.

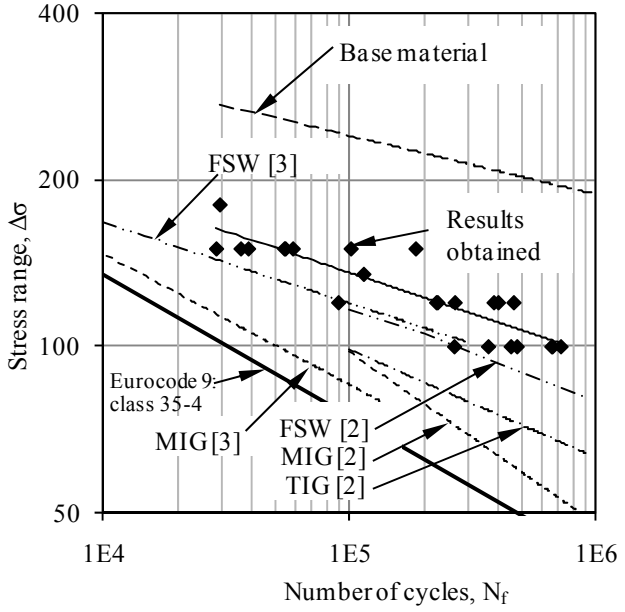

Figure 11. S-N curves for aluminium alloy AA 6082-T6 under constant amplitude loading. R=0.

Fatigue results obtained in this work are close with data obtained by other authors for this welding process. FSW specimens show higher fatigue resistance than specimens welded by the other two processes (MIG and TIG). However, the friction stir welded specimens presented significantly lower lives than base material. Figure 12 shows the two typical crack initiation modes identified by optical observation, from the tunnel defect (Figure 12a) or at surface near stress concentration due to shear lips (figure 12 b).

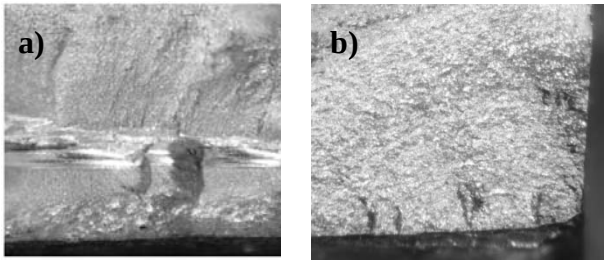

Figure 12. Fatigue crack initiation modes identified in welded specimens.

Tunnel defects revealed to be more detrimental on fatigue resistance than stress concentration due to shear lips. Therefore, to reduce the difference between FSW welds and base material fatigue strengths is crucial to avoid the presence of tunnel defects. The higher fatigue resistance was obtained when axial force during welding process was well controlled, leading to a smooth upper surface and performing two welding passages in order to eliminate completely tunnel defects. A small loss of hardness resulting from the second welding passage was observed, however fatigue resistance was not significantly affected.

Comparing with Eurocode 9 design curve, FSW welds are clearly in the safe side, indicating that a higher class than 35-4 can be attributed to butt joints welded by FSW, providing that a good control of welding parameters is performed in order to avoid severe internal defects and that stress concentration near shear lips is minimized.

4. CONCLUSIONS

Friction stir welding process leads to a decrease of the material mechanical properties: yield and rupture stress are lower than for base material. Detailed examination revealed a hardness decrease in the thermo mechanically affected zone and the nugget zone average hardness was found to be significantly lower than the base alloy hardness.

The friction stir welded AA6082-T6 specimens presented significantly lower lives than base material specimens. Tunnel defects and shear lips, formed mainly in the retracting side, lead to a significantly reduction of the fatigue lives. Tunnel defects revealed to be more detrimental on fatigue resistance than stress concentration created near shear lips. The higher fatigue resistance was obtained when the axial force was well controlled in order to obtain a smooth upper surface, and performing two welding passages to eliminate completely tunnel defects.

A good agreement was observed between constant and variable amplitude fatigue tests, plotting equivalent stress, calculated accordingly to Miner´s rule, against the number of cycles to failure. The damage sum was ranged between 0,6 and 2 for the stress ratio R=0 under the four spectra loadings analysed. For R=-1 fatigue data obtained under variable amplitude presented lower lives than under constant amplitude loading, indicating that damage sum values are lower than unity for the majority of the tests. Therefore, Miner´s rule seems to overestimate fatigue life for R=-1.

REFERENCES

[1] Thomas, W. M., Nicholas, E. D., Needham, J. C., Much, M. G., Templesmith, P. und Dawes, C. J., G. B. patent application No. 9125978.8 (December 1991)..

[2] Ericsson, M., and Sandstrom, R., Influence of welding speed on the fatigue of friction stir welds, and comparison with MIG and TIG. International Journal of Fatigue 25 (2003)1379–1387

[3] Moreira, P.M.G.P, Jesus, A.M.P, Ribeiro, A.S. and Castro, P.M.S.T. *Fatigue crack growth in friction stir welds of 6082-T6 and 6061-T6 aluminium alloys: A comparison*. Theoretical and Applied Fracture Mechanics 50-2 (2008) 1-91.

[4] Lanciotti, A and Vitali, F. *Characterisation of friction stir welded joints in aluminium alloy 6082-t6 plates*. Welding International 17-8 (2003) 624-630.

[5] Kobayashi, Y., Sakuma, M., Tanaka Y and Matsuoka K. *Fatigue Strength of Friction Stir Welding Joints of Aluminium Alloy 6082 Extruded Shape*. Welding International 21-1 (2007) 18–24.

[6] Cavaliere, P., De Santis, A., Panella, F. and Squillace A. *Effect of welding parameters on mechanical and microstructural properties of dissimilar AA6082–AA2024 joints produced by friction stir welding*. Materials and Design 30 (2009) 609–616.

[7] Miner MA. *Cumulative damage in fatigue*. J Appl Mech 1945;12: A159–A64.

[8] Heuler P, Klatschke H. *Generation and use of standardized load spectra and load–time histories*. Int J Fatigue 27-8 (2005) 974–90.

[9] ASTM E739-91, *Standard Practice for Statistical Analysis of Linear or Linearized Stress-Life (S-N) and Strain-Life (ε-N) Fatigue Data*. E08.04, Book of Standards, vol. 03.01, Wset Conshohocken, USA.